Science of the Total Environment 566–567 (2016) 1489–1499

Contents lists available at ScienceDirect

Science of the Total Environment

journal homepage: www.elsevier.com/locate/scitotenv

A multi-radionuclide approach to evaluate the suitability of $^{239+240}$Pu as soil erosion tracer

Katrin Meusburger [a,*], Lionel Mabit [b], Michael Ketterer [c], Ji-Hyung Park [d], Tarjan Sandor [e,1], Paolo Porto [f], Christine Alewell [a]

[a] Environmental Geosciences, University of Basel, Bernoullistrasse 30, CH-4056 Basel, Switzerland
[b] Soil and Water Management and Crop Nutrition Laboratory, FAO/IAEA Agriculture & Biotechnology Laboratory, IAEA Laboratories, Seibersdorf, Austria
[c] Chemistry Department, Metropolitan State University of Denver, CO, USA
[d] Department of Environmental Science & Engineering, Ewha Womans University, Seoul 120-750, Republic of Korea
[e] Radioanalytical Reference Laboratory, Central Agricultural Office Food and Feed Safety Directorate, Hungary
[f] Dipartimento di AGRARIA, Università degli Studi "Mediterranea" di Reggio Calabria, Italy

HIGHLIGHTS

- The suitability of $^{239+240}$Pu as soil erosion tracer is compared to ^{137}Cs and ^{210}Pb$_{ex}$.
- $^{239+240}$Pu/^{137}Cs activity ratio indicates migration and preferential transport.
- As such it is proposed as a proxy for the particle size correction factor.
- The new conversion model MODERN yields comparable erosion estimates.
- $^{239+240}$Pu appears as a promising alternative to the other radionuclide soil tracers.

GRAPHICAL ABSTRACT

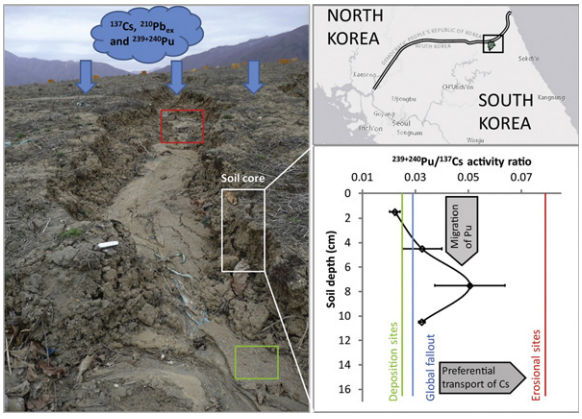

ARTICLE INFO

Article history:
Received 1 April 2016
Received in revised form 6 June 2016
Accepted 6 June 2016
Available online 20 June 2016

Editor: Jay Gan

Keywords:
Particle size correction factor
$^{239+240}$Pu/^{137}Cs activity ratio

ABSTRACT

Fallout radionuclides have been used successfully worldwide as tracers for soil erosion, but relatively few studies exploit the full potential of plutonium (Pu) isotopes. Hence, this study aims to explore the suitability of the plutonium isotopes ^{239}Pu and ^{240}Pu as a method to assess soil erosion magnitude by comparison to more established fallout radionuclides such as ^{137}Cs and ^{210}Pb$_{ex}$. As test area an erosion affected headwater catchment of the Lake Soyang (South Korea) was selected. All three fallout radionuclides confirmed high erosion rates for agricultural sites (>25 t ha^{-1} yr^{-1}). Pu isotopes further allowed determining the origin of the fallout. Both ^{240}Pu/^{239}Pu atomic ratios and $^{239+240}$Pu/^{137}Cs activity ratios were close to the global fallout ratio. However, the depth profile of the $^{239+240}$Pu/^{137}Cs activity ratios in undisturbed sites showed lower ratios in the top soil increments, which might be due to higher migration rates of $^{239+240}$Pu. The activity ratios further indicated preferential transport of ^{137}Cs from eroded sites (higher ratio compared to the global fallout) to the depositional sites (smaller ratio). As such

* Corresponding author.
E-mail addresses: Katrin.Meusburger@unibas.ch (K. Meusburger), L.Mabit@iaea.org (L. Mabit), mkettere@msudenver.edu (M. Ketterer), jhp@ewha.ac.kr (J.-H. Park), paolo.porto@unirc.it (P. Porto), Christine.Alewell@unibas.ch (C. Alewell).
[1] Present address: IAEA Laboratories Seibersdorf, Austria.

http://dx.doi.org/10.1016/j.scitotenv.2016.06.035
0048-9697/© 2016 The Authors. Published by Elsevier B.V. This is an open access article under the CC BY-NC-ND license (http://creativecommons.org/licenses/by-nc-nd/4.0/).

Conversion models
MODERN
$^{210}Pb_{ex}$
South Korea

the $^{239+240}Pu/^{137}Cs$ activity ratio offered a new approach to parameterize a particle size correction factor that can be applied when both ^{137}Cs and $^{239+240}Pu$ have the same fallout source. Implementing this particle size correction factor in the conversion of ^{137}Cs inventories resulted in comparable estimates of soil loss for ^{137}Cs and $^{239+240}Pu$. The comparison among the different fallout radionuclides highlights the suitability of $^{239+240}Pu$ through less preferential transport compared to ^{137}Cs and the possibility to gain information regarding the origin of the fallout. In conclusion, $^{239+240}Pu$ is a promising soil erosion tracer, however, since the behaviour i.e. vertical migration in the soil and lateral transport during water erosion was shown to differ from that of ^{137}Cs, there is a clear need for a wider agro-environmental testing.

© 2016 The Authors. Published by Elsevier B.V. This is an open access article under the CC BY-NC-ND license (http://creativecommons.org/licenses/by-nc-nd/4.0/).

1. Introduction

Both Caesium-137 (^{137}Cs) and excess Lead-210 ($^{210}Pb_{ex}$) radioisotopes have been used successfully worldwide as tracer for soil erosion assessment in the past decades (Mabit et al., 2014; Mabit et al., 2013; Porto and Walling, 2012a; Porto et al., 2013). Because of the technical limitations associated to the determination of $^{210}Pb_{ex}$ as well as the fact that only around 30% of the deposited ^{137}Cs global fallout is still present due to its radioactive decay (Mabit et al., 2013; Mabit et al., 2014), the quest for new fallout radionuclide (FRN) soil tracers has directed the attention of the scientific community to the use of plutonium (Pu) isotopes. To date, however, there have been relatively few attempts to exploit the full potential of plutonium (Pu) isotopes as soil erosion tracers. Indeed, Pu was found to be highly particle-reactive and hence binds even more effectively to soil particles than ^{137}Cs (Hakonson et al., 1981). Furthermore, due to much longer half-lives compared to ^{137}Cs and ^{210}Pb ($t_{1/2}$ = 30.2 and 22.3 years, respectively) of Pu isotopes (i.e. ^{239}Pu $t_{1/2}$ = 24,110 years and ^{240}Pu $t_{1/2}$ = 6561 years) their sensitivity does not decline (Everett et al., 2008). Even though Schimmack et al. (2001) already discussed the advantages of $^{239+240}Pu$ compared to ^{137}Cs, it was not until the advent of the less time-consuming inductively coupled plasma mass spectrometry (ICP-MS) for $^{239+240}Pu$ analysis that the potential advantages of Pu isotopes could be used for soil erosion assessment (Alewell et al., 2014; Ketterer et al., 2002; Lal et al., 2013; Tims et al., 2010; Xu et al., 2013; Yamada et al., 2006). As such, studies dealing with the assessment of soil erosion and deposition in agro-ecosystems using Pu are limited to a few applications performed in Australia, China, Germany, and Switzerland (Alewell et al., 2014; Everett et al., 2008; Schimmack et al., 2001; Tims et al., 2010; Xu et al., 2013; Xu et al., 2015; Zollinger et al., 2014).

Like ^{137}Cs, $^{239+240}Pu$ fallout originates from the thermonuclear weapons testing that took place from the mid-1950s to the early 1960s, or from nuclear power plant (NPP) accidents such as Chernobyl in April–May 1986 and Fukushima in March–April 2011 (Liao et al., 2014). Further the Chinese and North Korean nuclear tests and yellow dust events (i.e. dust clouds leaving the mainland of China and traveling towards Korea and Japan) can be expected as potential contributing sources for ^{137}Cs and $^{239+240}Pu$ in our chosen catchment (Haean) in South Korea (Hirose et al., 2004; Yamada et al., 2006). In contrast, excess ^{210}Pb ($^{210}Pb_{ex}$) is a natural geogenic radioisotope originating from the decay of ^{226}Ra, which is found in most soils and rocks and which produces short-lived gaseous ^{222}Rn ($t_{1/2}$ = 3.8 days) as its daughter. Most of this ^{222}Rn decays to ^{210}Pb within the soil, producing supported ^{210}Pb, which is in equilibrium with its ^{226}Ra parent. Some of the ^{222}Rn diffuses from the soil into the atmosphere, where it rapidly decays to ^{210}Pb. This ^{210}Pb is deposited as fallout and since it is not in equilibrium with the parent ^{226}Ra, it is commonly termed unsupported or excess $^{210}Pb_{ex}$. Because of its natural origin, the atmospheric flux of $^{210}Pb_{ex}$ is essentially constant through time, although seasonal and longer-term variations have been identified (Preiss et al., 1996).

There are two main limitations in using $^{239+240}Pu$ to investigate soil redistribution in agro-ecosystems. One is the lack of suitable conversion models allowing for the conversion of Pu areal activities into soil redistribution rates. Different mathematical conversion models are available, which in case of ^{137}Cs and $^{210}Pb_{ex}$ are well validated (Porto and Walling, 2012a; Porto and Walling, 2012b; Porto et al., 2003), but the applicability of these models to $^{239+240}Pu$ has not been tested yet. So far, Pu conversion models assume either an exponential depth distribution in the soil such as the inventory model of Lal et al. (Lal et al., 2013) or homogenous mixing within the plough layer as in mass balance models (Xu et al., 2013; Zhang et al., 2015). The second major uncertainty when using $^{239+240}Pu$ is related to its different mobility compared to ^{137}Cs within the soil profile but also with respect to preferential transport during soil erosion. The preferential loss of ^{137}Cs during soil erosion is well-known, but rarely corrected by implementing a site specific particle size correction factor. Whether $^{239+240}Pu$ is also preferentially eroded has, according to our knowledge not been studied yet.

The general objective of this study is to evaluate the suitability of $^{239+240}Pu$ as a tracer for quantifying soil erosion under different land use. In addition to previous studies using $^{239+240}Pu$ as soil erosion tracer we will focus on the above mentioned limitations regarding i) the suitability of different conversion models for $^{239+240}Pu$ conversion and ii) the differing mobility of $^{239+240}Pu$ and ^{137}Cs. We adopted a multi-radionuclide approach and will compare $^{239+240}Pu$ based soil erosion estimates to those of more established FRNs such as ^{137}Cs and $^{210}Pb_{ex}$. The use of FRNs has been discussed with regard to their applicability and reliability (Mabit et al., 2013; Parsons and Foster, 2011) and as such a rigorous comparison among different FRNs regarding the suitability to trace soil erosion on different land use types is presented. Moreover, in context of the applicability of conversion models the newly introduced model MODERN (i.e. Modelling Deposition and Erosion rates with RadioNuclides) that allows deriving soil erosion/sedimentation rates from any FRNs content (Arata et al., 2016a; Arata et al., 2016b) will be evaluated. To investigate the different mobility, we utilize the $^{240}Pu/^{239}Pu$ atomic ratios and $^{239+240}Pu/^{137}Cs$ activity ratios to determine the origin of the ^{137}Cs and $^{239+240}Pu$ fallout as well as to indicate their different susceptibility to vertical migration in the soil profile and to preferential transport during water erosion processes.

2. Materials and method

2.1. Study area

The investigated study site is located within the Haean catchment (Fig. 1), adjacent south of the demilitarized zone (DMZ), South Korea (N 38 15′, E 128 15′). The Haean catchment was selected because it is a multiple land-use catchment, where several case studies have reported high rates of soil erosion associated with intensive cultivation of vegetables and ginsengs on agricultural lands converted from forest on steep slopes (Arnhold, 2012; Ruidisch et al., 2013a).

The catchment is under temperate climate conditions with mean annual precipitation of 1599 mm (13 year average from 1999 to 2011), with 45% of the annual rainfall occurring in June and July, associated with the Asian monsoon (Jung et al., 2012). These intense monsoon events are highly erosive (Arnhold et al., 2014). The mean annual temperature is 8.5 °C (1999–2011) and ranges from −6.8 °C in January to 21.5 °C in July.

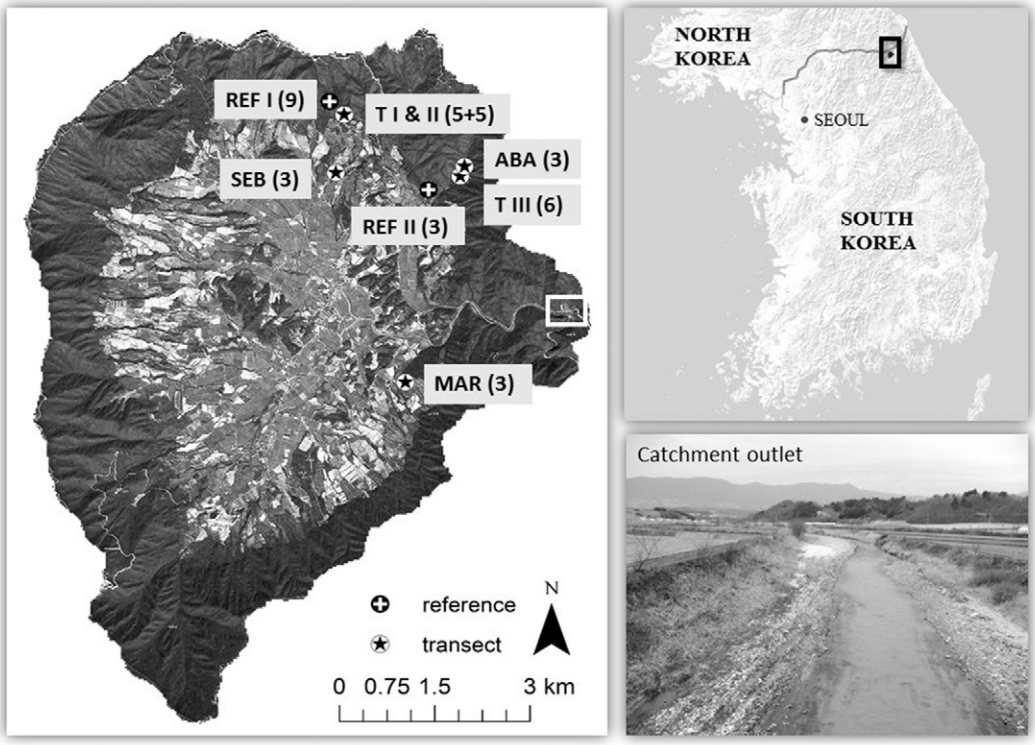

Fig. 1. Haean catchment with location of the reference sites (REF I and REF II) and sample transects. Numbers in the brackets indicate the soil profiles taken per site.

The parent material in the basin bottom consists of highly weathered biotite granites. The dominant soil types are Anthroposols and Arenosols. The surrounding mountain ridges are of metamorphic rock (Kwon et al., 1990) mainly forming acidic and podzolic Cambisols. The characteristic bowl-shaped topography (400–1304 m a.s.l.) of the catchment causes a subdivision into three major land use zones: steep forested hillslopes (58%), moderate slopes with dryland farming (22%) and flat rice paddies (8%) (Ruidisch et al., 2013b). On the dryland fields, the main crops are cabbage, radish, potato, and beans. Particularly during their early growth stages, these crops are susceptible to soil erosion because of the low ground cover. The commonly applied agricultural practice, the ridge tillage with polyethylene covers, further enhances soil erosion and rapidly leads to land degradation (Ruidisch et al., 2013a). To counteract soil losses and increase fertility, the farmers add topsoil from nearby forests to their agricultural fields. The intensive agriculture along with the highly erodible soils developed from saprolites at the basin bottom constitutes the major source of suspended sediment to the drinking water reservoir Lake Soyang (Park et al., 2011).

2.2. Soil sampling and laboratory analysis

In April 2010, a total of 37 soil profiles (until reaching the bedrock) were collected with a soil corer of 59 mm diameter and 90 cm in length (Giddings Machine Company, Windsor, CO, USA). We selected 6 transects and two reference sites for our investigation (Fig. 1). Transect I and II (T I and T II) were located at steep forested slopes (with 5 sampling points each) Three other transects (with three sampling points each) were located on cultivated fields: one intensely used cabbage field (abbreviated with SEB), one abandoned field (abbreviated with ABA) and a recently deforested field where maize was grown since 2006 (abbreviated with MAR). Another slope transect (T III) includes 6 sampling points from the forest (upslope) to an arable field (downslope).

Taking into account the risk associated with the sampling campaign in the mined area, two representative reference sites were selected on flat, forested ridge tops. For each site three soil profiles were taken as 3 cm depth incremental samples. In addition, we extracted 6 soil profiles at the reference site 1 that were measured as bulk sample. The suitability of these reference sites was confirmed by the $\delta^{13}C$ and $\delta^{15}N$ stable isotope soil profiles (Meusburger et al., 2013). Prior to the radioisotopic analysis, the soil samples were dried for three days at 40 °C. This low temperature was selected to not affect the carbon stable isotope signal of the soil samples. Afterwards, the soil was passed through a 2 mm sieve to remove stones and was ground with a tungsten carbide swing grinder for homogenization.

Gamma spectrometry was used for the measurement of ^{137}Cs and the determination of $^{210}Pb_{ex.}$ The ^{137}Cs was measured at 662 keV. The determination of $^{210}Pb_{ex}$ (unsupported ^{210}Pb) activity required the measurement of total ^{210}Pb activity and ^{226}Ra activity, which is equivalent to the supported ^{210}Pb fraction: $^{210}Pb_{ex} = {}^{210}Pb_{total} - {}^{226}Ra$. ^{226}Ra was measured by gamma spectrometry via the gamma ray energies of its daughters ^{214}Bi and ^{214}Pb, at 609 keV and 351 keV, respectively. Assessing ^{226}Ra using its daughters ^{214}Pb or ^{214}Bi by gamma spectrometry, equilibrium with its direct gaseous daughter ^{222}Rn is required. To achieve equilibrium between ^{226}Ra and ^{222}Rn, soil samples were sealed for 21 days prior to performing gamma analysis, to avoid the escape of radon.

The ^{137}Cs and ^{210}Pb activities in soil samples were determined using a N′-type high purity HPGe detector (8 k, CANBERRA Multiport; 30% relative efficiency; energy range 20–2000 keV) with a CARBON-EPOXY window shielded with 10 cm high purity lead and 3 mm copper. The counting time for each sample was set at 80,000 s to reach an acceptable level of detection limit. The software used for peak evaluation was Winner 6.0. Calibration of equipment, analysis and quality control of the measurements were performed following IAEA standard procedure (Shakhashiro and Mabit, 2009).

The measurement of Plutonium isotopes ($^{239+240}Pu$) activity was performed at Northern Arizona University using a Thermo X Series II quadrupole ICP-MS. The ICP-MS instrument was equipped with a high-efficiency desolvating sample introduction system (APEX HF, ESI

Scientific, Omaha, NE, USA). A detection limit of 0.1 Bq kg^{-1} for $^{239+240}$Pu was obtained for samples of nominal 1 g of dry-ashed material; for $^{239+240}$Pu activities >1 Bq kg^{-1}, the measurement error was 1–3%. Prior to mass spectrometry analysis, the samples were dry-ashed and spiked with ~0.005 Bq of a ^{242}Pu yield tracer (obtained as a licensed solution from NIST). Pu was leached with 16 M nitric acid overnight at 80 °C, and was subsequently separated from the leach solution using a Pu-selective TEVA resin (Ketterer et al., 2011). The masses of ^{239}Pu and ^{240}Pu present in the sample were determined by isotope dilution calculations and then converted into the summed $^{239+240}$Pu activity.

2.3. Conversion of fallout radionuclide inventories to soil redistribution rates and introduction of the new conversion model MODERN

The mass activities of the FRNs (Bq kg^{-1}) were converted into areal activities also termed inventories (Bq m^{-2}) with measured mass depth (xm) of fine soil material (kg m^{-2} sampling $depth^{-1}$). The use of FRN measurements to quantify soil redistribution magnitude is commonly based upon the comparison of FRN inventories for individual sampling points to a local reference inventory. The inventory change (Inv_{change}) was calculated as:

$$Inv_{change} = \frac{Inv - Inv_{ref}}{Inv_{ref}} \times 100 \quad (1)$$

where Inv_{ref} is the local reference total inventory as mean of all reference sites (Bq m^{-2}) and Inv is measured total inventory at the sampling point (Bq m^{-2}). Negative values of Inv_{change} indicate erosion, whereas positive values indicate deposition.

When FRNs reach the soil surface by wet deposition, they are tightly adsorbed to fine soil particles. The subsequent lateral redistribution of adsorbed FRN is associated with soil erosion. Soil erosion is indicated by lower FRN inventories, while sedimentation is indicated by higher FRN inventories compared to the reference site (Mabit et al., 2008). The conversion of FRN inventories to soil erosion/deposition rates requires different conversion models depending on the land use and the FRN being used (Table 1). A detailed description of each conversion model used is provided in the supplementary material. Only the recent model MODERN (Modelling Deposition and Erosion rates with RadioNuclides) will be introduced below. MODERN can be applied for cultivated and uncultivated sites and all FRNs presented here. Instead of using a distinct function to describe the depth distribution of the FRNs in the soil, this model works iteratively and as such does not depend on an exponential FRN depth distribution but is able to describe any specific depth distribution of a soil. MODERN rebuilds the depth profile of the reference sites as a step function $g(x)$, which at each increment inc returns the value Inv (inc). Finally, Inv is the total inventory of a sampling site, measured for the whole of depth d (cm).

The model targets at the level x^*(cm), where the cumulated value of the inventory of the reference site, from x^* to $x^* + d$ (cm), is equal to Inv. Therefore x^* should fulfil the following equation:

$$\int_{x^*}^{x^*+d} g(x)dx = Inv \quad (2)$$

To obtain all possible solutions, simulated layers of 3 cm (our resolution of the depth incremental samples) each, are added below (in case of erosion) and above (in case of deposition) the reference profile, to assess potential soil losses or gains. The new simulated depth profile is described by the function S, where:

$$S(x) = \int_{x}^{x+d} g(x')dx' \quad (3)$$

The function S can be represented through the primitive function F of the distribution function g(x) as follows:

$$S(x) = F(x+d) - F(x) \quad (4)$$

Independent of the model used, the assessment of sedimentation rates always requires information of the sediment source horizon. Thus, to derive sedimentation rates, assumptions about the upslope eroding area and the thickness of the soil layer affected is needed. For instance, a high inventory at a sampling site could be the result of a high sedimentation rate from source horizons with low FRN activity or a relatively low amount of soil with high FRN activity. To account for this uncertainty we applied two different scenarios of the simulated sedimentation layers: (i) each of the layers deposited trough sedimentation processes contains the same inventory as the top layer of the reference site, (ii) the layer with the maximum activity was eroded. Both scenarios result in rather conservative sedimentation rates, because only source horizons with a relatively high FRN content are considered. As such much higher sedimentation rates are likely if deeper soil layers are contributing to the sediment yield.

Table 1
Conversion models used for assessing soil redistribution in cultivated and uncultivated agricultural sites using different fallout radionuclides (DMM = Diffusion and Migration Model; IM = Inventory Model; MBM = Mass Balance Models; MODERN = Modelling Deposition and Erosion rates with RadioNuclides; PDM = Profile Distribution Model; * indicated models used for the comparison of soil redistribution rates of different fallout radionuclides).

FRNs	Cultivated site	Uncultivated site
^{137}Cs	• MBM2* (Walling et al., 2002; Walling et al., 2014) • MODERN (Arata et al., 2016a, 2016b)	• PDM* (Walling et al., 2002; Walling et al., 2014) • DMM (Walling et al., 2002; Walling et al., 2014) • MODERN (Arata et al., 2016a, 2016b)
$^{210}Pb_{ex}$	• MBM1 (Walling et al., 2002; Walling et al., 2014) • MBM2 (Walling et al., 2002; Walling et al., 2014) • MODERN* (Arata et al., 2016a, 2016b)	• DMM (Walling et al., 2002; Walling et al., 2014) • MODERN* (Arata et al., 2016a, 2016b)
$^{239+240}$Pu	• Simplified MBM (Xu et al., 2015) • MODERN* (Arata et al., 2016a, 2016b)	• IM (Lal et al., 2013) • MODERN* (Arata et al., 2016a, 2016b)

3. Results and discussion

3.1. ^{240}Pu/^{239}Pu atomic ratios and $^{239+240}$Pu/^{137}Cs activity ratios

The measured ^{240}Pu/^{239}Pu atomic ratios at our study sites varied from 0.159 to 0.215 with an average of 0.182 ± 0.015. The measured ^{240}Pu/^{239}Pu ratios agree well with the integrated atmospheric fallout value of 0.18 ± 0.014 (Kelley et al., 1999). This implies that the main source of Pu in our samples is the global atmospheric fallout and does not point out a potential contribution from nuclear activities in North Korea. The latter is congruent with other studies concluding that no volatile radionuclides from the nuclear weapon testing have yet been observed in South Korea, Japan or China (Xu et al., 2013). Another potential source for Pu is the nuclear weapons testing conducted in Lop Nor (Xinjiang region, northwest China) after the 1963 nuclear test-ban treaty. In the study of Liao et al. (2014) a sediment sample from Lake Bosten (lake closest to the Lop Nor Chinese Nuclear Weapon Test site established in October 1959) indicated a low ^{240}Pu/^{239}Pu atom ratio of 0.08 for these tests. However, due to the long distance between our sites and Lop Nor, such fallout seems unlikely.

The $^{239+240}$Pu/^{137}Cs activity ratios (corrected to 1.7.1998) for the bulk reference samples are on average 0.032 ± 0.017 (Fig. 2 a, solid line). They lie within the reported global fallout ratio of 0.029 ± 0.003, but show considerably higher variation (Hardy et al., 1973; Hodge

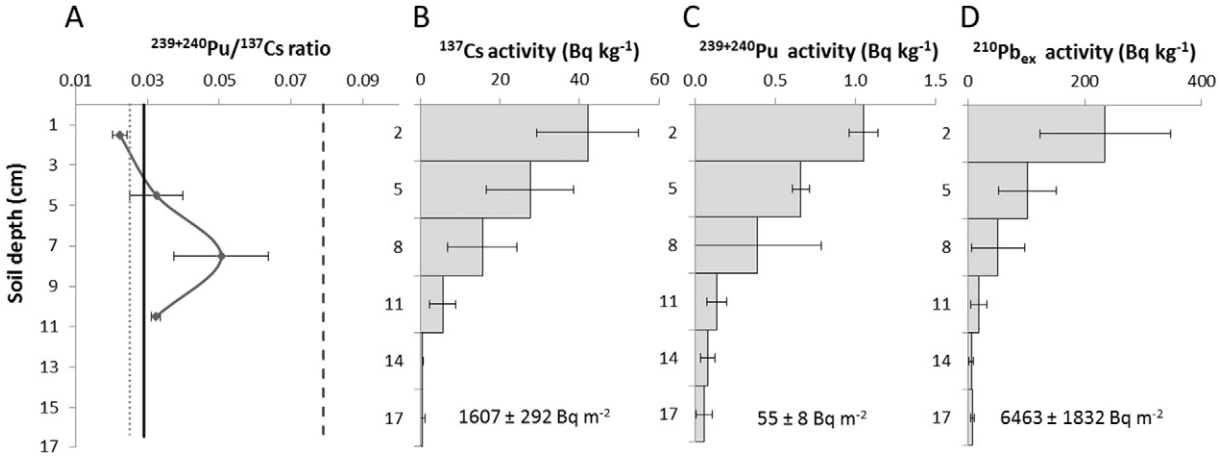

Fig. 2. a) $^{239+240}Pu/^{137}Cs$ activity ratios for the six reference soil profiles with the vertical lines indicating the global fallout ratio (solid), the ratio of sedimentation sites (points) and erosion sites (dashed). Average vertical distributions of ^{137}Cs (b), $^{210}Pb_{ex}$ (c) and $^{239+240}Pu$ (d) in the reference site. X-error bars correspond to the standard deviation values (n = 6). For visibility Y-error bars are not shown, but correspond to 3 cm which is the resolution of soil sample increments.

et al., 1996; Kelley et al., 1999). $^{239+240}Pu/^{137}Cs$ for the Chinese nuclear tests is so far unknown and ratios for the Chernobyl and the Fukushima Daiichi Nuclear Power Plant accident were very different with ratios of about 0.009 and 6.76×10^{-8}, respectively (Liao et al., 2014). The higher variation observed for our sites is most likely explained through the different adsorption behaviour of $^{239+240}Pu$ and ^{137}Cs in the soil. As illustrated in Fig. 2 b, c, d the upper 12 cm of the soils contain 98%, 92%, and 94% of the ^{137}Cs, $^{239+240}Pu$, and $^{210}Pb_{ex}$ inventory, respectively. But relatively low activity ratios and thus higher amounts of ^{137}Cs compared to the global $^{239+240}Pu/^{137}Cs$ fallout ratio occur in the upper part of the soil profile and relatively high ratios and low amounts of ^{137}Cs in the deeper layers. The latter implies a higher mobility and migration rate of $^{239+240}Pu$ compared to ^{137}Cs under our site conditions.

$^{239+240}Pu$ in soils is associated mainly with organic matter and sesquioxides whereas ^{137}Cs is known to be mostly bound to the fine mineral fraction (Lujaniene et al., 2002; Qiao et al., 2012). Consequently a relatively higher proportion of $^{239+240}Pu$ is exchangeable and might migrate downward the soil. Compared to ^{137}Cs, the migration of $^{239+240}Pu$ into the soil is enhanced particularly if changes in pH and/or decomposition of organic matter occurs and the dissolved organic carbon (DOC) in the runoff will transport more Pu since dissolved humic substances bind Pu by complexation much stronger than Cs (Choppin, 1988; Lu et al., 1998; Lujaniene et al., 2002; Qiao et al., 2012). Thus, $^{239+240}Pu$ generally has its peak concentration slightly below the top-soil surface whereas for ^{137}Cs an exponential decline with soil depth is more common (Alewell et al., 2014; Xu et al., 2013). The Korean $^{239+240}Pu$ and ^{137}Cs soil profiles obtained in the framework of our study confirm these previous observations made in Northeast China and in the Swiss Alps (Alewell et al., 2014; Xu et al., 2013).

Even though $^{239+240}Pu$ and ^{137}Cs seem to have a different migration behaviour in the soil, these processes are relatively slow and a significant correlation between $^{239+240}Pu$ and ^{137}Cs activity remains, which is in correspondence with other studies (Kim et al., 1998; Lee et al., 1997; Xu et al., 2013). Compared to $^{239+240}Pu$, $^{210}Pb_{ex}$ is mainly adsorbed by organic matter but also by clay-sized mineral particles such as ^{137}Cs. At our sites the average depth profiles of all three FRNs show an exponential decrease with soil depth (Fig. 2) and the three isotopes are strongly correlated (Spearman rank correlation $r > 0.96$). Exponential fits to the measured activity against the mass depth yield R^2 values above 0.9 in all cases (0.99 for ^{137}Cs, 0.94 for $^{210}Pb_{ex}$ and 0.92 for $^{239+240}Pu$). In the case of $^{239+240}Pu$, the high R^2 is slightly misleading since $^{239+240}Pu$ clearly migrated deeper into the soil (Fig. 2a). $^{239+240}Pu$ reaches deepest into the soil and even though the activity in the uppermost layer is largely overestimated by the exponential fit it does not present the often-observed subsurface activity peak (Alewell et al., 2014; Lal et al., 2013; Tims et al., 2010; Xu et al., 2015).

The $^{239+240}Pu$ activities in the top soil layers (0–3 cm) of the three reference soil cores were in the range of 0.92 to 1.1 Bq kg^{-1}, agreeing well with the published values of 0.18 to 1.85 Bq kg^{-1} for top soil layers (0–5 cm) in South Korea (Kim et al., 1998) and the 0.47 to 1.62 Bq kg^{-1} levels recorded in China at similar latitudes (Xu et al., 2015).

3.2. Estimation of ^{137}Cs particle size factor from $^{239+240}Pu/^{137}Cs$ activity ratios

Another interesting aspect of the $^{239+240}Pu/^{137}Cs$ activity ratios is their difference for bulk soil samples collected at potentially disturbed sites which differ ($p = 0.07$; *t*-test) between sites affected by erosion and sedimentation processes with ratios of 0.079 ± 0.088 and 0.025 ± 0.006, respectively (dashed and dotted line in Fig. 2a). Compared to the global fallout ratio established in the local reference, the erosion sites are depleted in ^{137}Cs and the sedimentation sites slightly enriched. The sedimentation sites show a lower variability of the ratio, which might be due to mixing of the eroded top soil material during the transport. The differing ratios between erosion and sedimentation sites indicate that during erosion ^{137}Cs might be mobilized prior to $^{239+240}Pu$ and/or to a larger extend. This could be due to a preferential transport of fine soil particles, where the major proportion of ^{137}Cs is adsorbed to. As such the differing ratio between reference, erosion and deposition sites, support the conclusions of Schimmack et al. (2001) that $^{239+240}Pu$ and ^{137}Cs do not behave identically during soil redistribution processes (erosion, transport and sedimentation). Pu reflects more than Cs the fate of the organic matter during erosion due to its strong binding to soil organic matter (Schimmack et al., 2001). The preferential transport of ^{137}Cs is well known and commonly result in relatively higher estimates of soil redistribution if no particle size correction is applied. The particle size correction factor (*P*) is usually added in conversion models to account for the selectivity of soil redistribution processes and its value can be expressed, as proposed by He and Walling (1996), as:

$$P = \left(\frac{S_{ms}}{S_{sl}}\right)^{v} \quad (2)$$

where S_{ms} is the specific surface area of mobilized sediment ($m^2\ g^{-1}$); S_{sl} is the specific surface area of the source soil ($m^2\ g^{-1}$) and *V* is a constant with a value of ~0.65 (He and Walling, 1996).

For a sedimentation site

$$P' = \left(\frac{S_{ds}}{S_{sl}}\right)^{v} \quad (3)$$

where S_{ds} is the specific surface area of the deposited sediment ($m^2\ g^{-1}$). Most often there is no information on the specific surface area of the sediments involved. Grain size composition of mobilized sediment is usually enriched in fines compared with the original soil, thus the correction factor is generally greater than 1.0. For a depositional site on the other hand, which is frequently depleted in fine fractions, the value of the correction factor is generally less than 1.0. As such and in analogy to the approach of He and Walling (1996), we suggest assessing the particle size correction factor using the $^{239+240}Pu/^{137}Cs$ activity ratios as a proxy. Based on the assumption that under the local condition of our study area $^{239+240}Pu$ is less sensitive to erosional preferential transport than ^{137}Cs, the relative depletion/enrichment of ^{137}Cs can be assess via the activity ratio by replacing the specific surface area with the $^{239+240}Pu/^{137}Cs$ activity ratios of the respective sediment involved. In case of the erosional site we divide the ratio of the erosional site by the one of the source soil and yield a particle size correction factor of $P = 0.079/0.032 = 2.47$. In case of the depositional site the ratio of the depositional site is divided by the source soil resulting in $P' = 0.025/0.032 = 0.78$. If we consider the empirical exponent of 0.65 proposed by He and Walling (1996) the values correspond to $P = 2.47\text{^}0.65 = 1.8$ and $P' = 0.78\text{^}0.65 = 0.85$. These P values are site specific and apply solely for ^{137}Cs under the assumption that no preferential transport of $^{239+240}Pu$ occurs during the erosion process, but the approach in general is expected to be applicable in any other catchment. Iurian et al. (2014) found particle size correction factors in a comparable range of P from 1 to 1.67 and P' from 0.33 to 0.76. Particle size correction factors of our sites are particularly high because of the predominant silty sandy soil texture in the study site. As found in other studies (Iurian et al., 2014; Van Pelt et al., 2007) neglecting the particle size correction factor results in an overestimation of soil loss by water erosion.

Most likely $^{210}Pb_{ex}$ is also affected by preferential transport, but we could not assess a particle size correction factor in a similar manner, since the $^{210}Pb_{ex}$ fallout is continuous over time. As such any change in the $^{210}Pb_{ex}/^{137}Cs$ and $^{210}Pb_{ex}/^{239+240}Pu$ ratios as a result of preferential transport is masked by $^{210}Pb_{ex}$ fallout subsequent to the erosive event.

3.3. Establishment of FRN baseline inventories

As reported by Meusburger et al. (2013), a reliable ^{137}Cs baseline inventory using the 10 depth-incremental samples was established at 1607 ± 292 Bq m^{-2} (coefficient of variation (CV) of 18%) with an allowable error of 11% at the 90% confidence level (Table 2).

The $^{210}Pb_{ex}$ reference inventory values show a higher variability with a CV of 28% and a mean inventory of 6463 ± 1832 Bq m^{-2}. The spatial variability of the reference inventories is within the range reported by Sutherland (1991, 1996), He and Walling (1996) and Teramage et al. (2015) for forest sites, and considerably lower as reported for a Japanese cypress plantation by Fukuyama et al. (2008) who found a CV of 61% and 68% for ^{137}Cs and $^{210}Pb_{ex}$, respectively. The annual fallout of $^{210}Pb_{ex}$ as well as the resulting soil inventories are reported to vary at global scale from 23 to 367 Bq $m^{-2}\ yr^{-1}$ and 1508 Bq m^{-2} for a flat crest in northern California (O'Farrell et al., 2007) to 19,703 Bq m^{-2} at Shimanto River basin, in southern Japan (Wakiyama et al., 2010).

For $^{239+240}Pu$, the reference inventory is estimated at 55 ± 8 Bq m^{-2} with a CV of 15%. Due to the influence of wind and pressure zones, the global redistribution of $^{239+240}Pu$ fallout resulted in an approximately similar deposit in areas located at the same hemispheric latitude (UNSCEAR, 2000). Our estimated reference inventory is within the range of expected $^{239+240}Pu$ global fallout under the 40–50°N latitudes i.e. 58.1 ± 18.5 Bq m^{-2} (UNSCEAR, 2000). Moreover, the average topsoil (0–3 cm) activity for our reference site (i.e. 1.05 Bq kg^{-1}) is within the upper range of the Korean topsoil activities of 0.24 to 1.1 Bq kg^{-1} reported by Lee et al. (1997).

Table 2
Descriptive statistic for the reference inventories of ^{137}Cs, $^{210}Pb_{ex}$ and $^{239+240}Pu$. SD = standard deviation; AE = allowable error at the 90% confidence level; CV = coefficient of variation.

Sample	^{137}Cs			Inventories (Bq m^{-2})			$^{239+240}Pu$		
				$^{210}Pb_{ex}$					
R1	1913	±	173	6661	±	1142	54.9	±	3.2
R2	1312	±	150	5184	±	1244	41.9	±	1.6
R3	1044	±	120	6115	±	1073	52.7	±	4.5
R4	1808	±	164	9940	±	1150	59.4	±	4.3
R5	1457	±	155	5623	±	1228	55.6	±	2.9
R6	1688	±	217	8951	±	1599	51.4	±	3.0
R7	1980	±	151	(−603	±	265)	49.4	±	2.0
R8	1732	±	266	5590	±	2591	64.2	±	3.0
R9	1717	±	263	5860	±	1980	70.6	±	2.2
R10	1420	±	250	4244	±	2126	48.3	±	2.3
Mean	1607	±	191	6463	±	1440	55	±	3
SD	292			1832			8		
AE	0.11			0.18			0.09		
CV	0.18			0.28			0.15		

Most of the collected samples in the steep forested slopes and the cultivated fields investigated exhibit a lower inventory compared to the respective reference inventories of each FRN highlighting the dominance of erosive processes and net soil loss budget. Nonetheless, both ^{137}Cs and $^{239+240}Pu$ indicate that for a few sampled sites sedimentation predominates. $^{210}Pb_{ex}$ was below the detection limit for most of the samples collected in the investigated sites. The latter might not only be related to low inventory values but also to the bulking of large soil volumes, which potentially diluted the $^{210}Pb_{ex}$ activity below the analytical detection limit. With respect to the high uncertainty related to the determination of $^{210}Pb_{ex}$ (see for e.g. Mabit et al., 2014), we strongly suggested for future soil redistribution studies to establish $^{210}Pb_{ex}$ depth incremental content not only for the reference sites but also at the sampled agricultural and forested sites.

3.4. Assessment of soil redistribution rates

3.4.1. Comparison of the results provided by the different conversion models

In a former study, ^{137}Cs based soil erosion rates for the uncultivated forest sites were assessed with the PDM (Meusburger et al., 2013). These previous reported results compare well ($R^2 = 0.98$; $p < 0.0001$) to estimates obtained using DMM (data not shown). Even better correspondence can be observed for the PDM and MODERN (Fig. 3 a; $p < 0.0001$). For the cultivated sites, MODERN agrees less to the MBM2 output ($R^2 = 0.63$; $p < 0.005$; Fig. 3 b). This is basically due to the site MAR1 where cultivation started only recently in 2006. Excluding this site (filled dot in Fig. 3 b) results in an almost 1:1 correspondence of MODERN and the MBM2 ($y = 1.096x–6.826$; $R^2 = 0.86$; $p < 0.0001$). MODERN does not account for the start date of the tillage yet, which might be the reason for the observed deviation in sites with a more recent tillage start date. However, overall the ^{137}Cs based soil erosion rates of MODERN compare well to the ones of the established conversion models.

In case of $^{239+240}Pu$, we applied the exponential Inventory Model (IM) proposed by Lal et al. (2013). We observed a close relation between the IM and MODERN for uncultivated sites ($R^2 = 0.90$, $p < 0.0001$), however, the erosion estimates based on the IM were twice as high (Fig. 3 c). The latter is most likely due to an overestimation of the surface soil concentration by the exponential function of the IM (Fig. S1, supplementary material).

For the cultivated sites, the MBM introduced by Xu et al. (2015) also resulted in considerably higher soil redistribution assessments (Fig. 3 d). The MBM is very insensitive to changes in the Pu inventory (in our

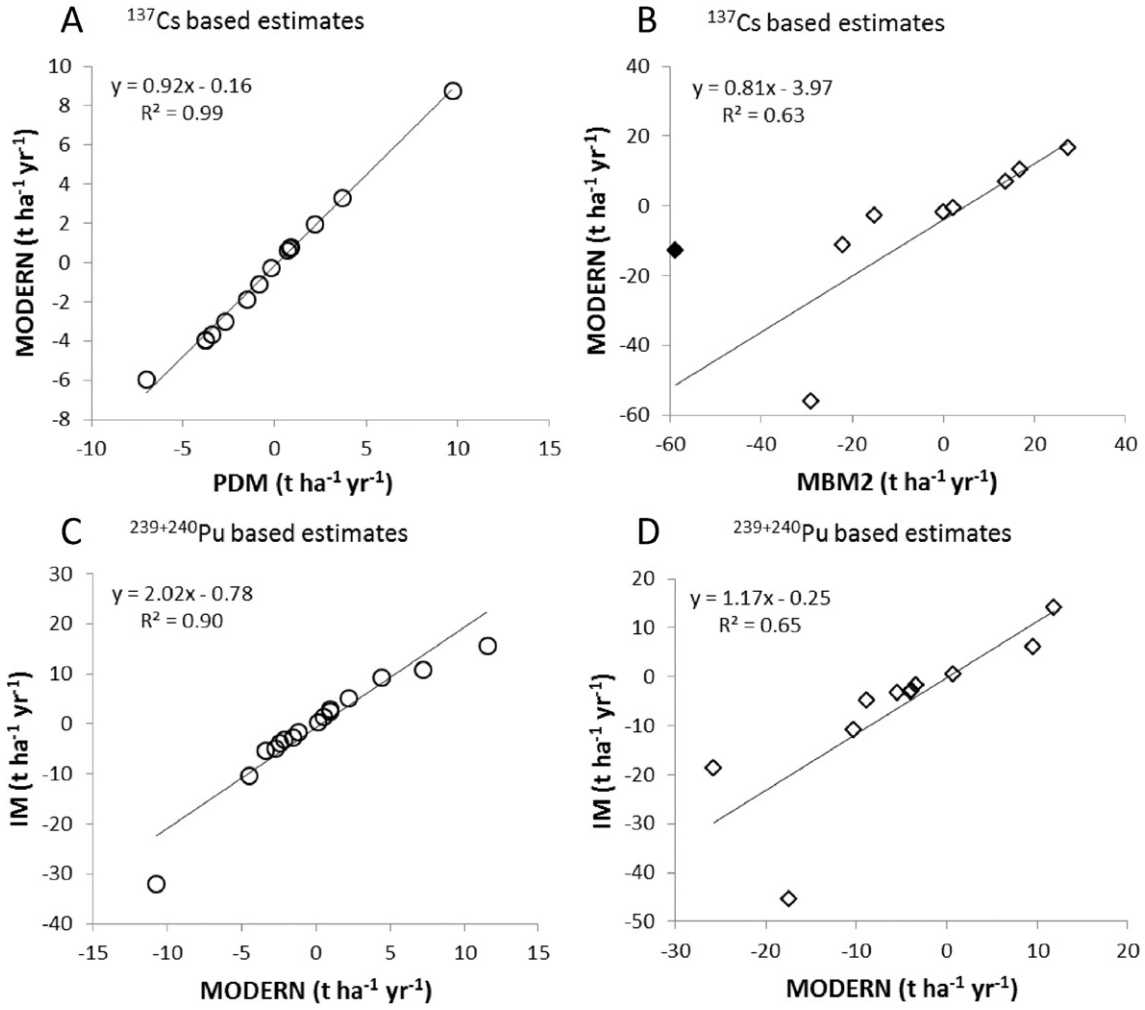

Fig. 3. ^{137}Cs based soil redistribution estimates calculated with the PDM for uncultivated sites (A) and the MBM2 for the cultivated sites (B) against MODERN estimates. $^{239+240}$Pu based soil redistribution estimates calculated with the Inventory Model (IM) for uncultivated sites (C) and the Mass Balance Model for the cultivated sites (D) against MODERN estimates. Positive values correspond to sedimentation rates, negative values to erosion rates.

case a site with 20% and 70% inventory loss yielded almost identical erosion rates of 27. 3 and 27.8 t ha^{-1} yr^{-1}, respectively). MODERN is not yet considering the start of the tillage in the conversion process. However, it enables to convert Pu inventories to soil redistribution rates for both cultivated and uncultivated sites. This is evident from the relationship between MODERN and the other well-established

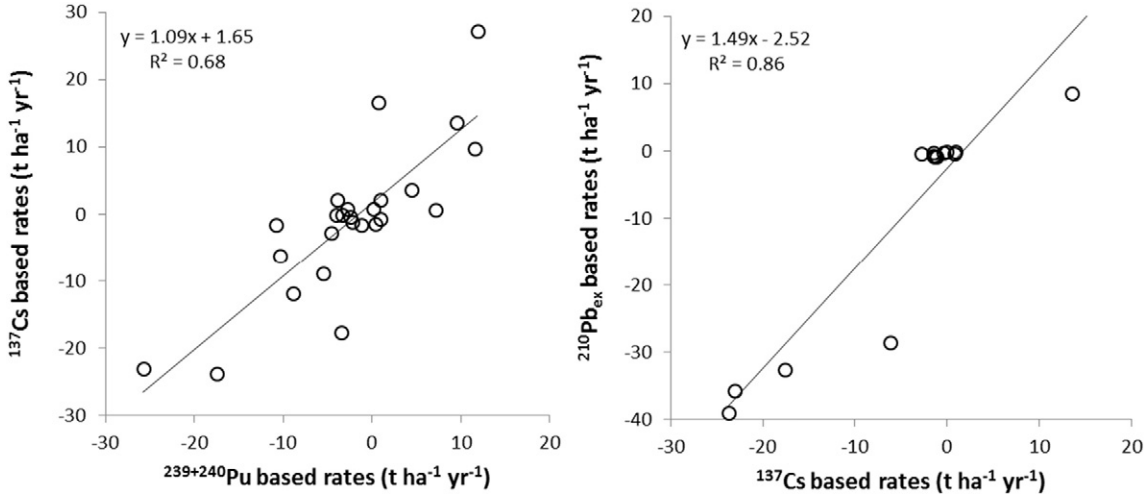

Fig. 4. Comparison of soil erosion assessments based on different fallout radionuclides. $^{239+240}$Pu and $^{210}Pb_{ex}$ derived erosion rates have been assessed with MODERN and the ^{137}Cs erosion rates with the PDM for uncultivated and the MBM2 for cultivated sites.

models for ^{137}Cs (Fig. 3 a, b). Moreover, MODERN agrees well with the IM also for the cultivated sites ($y = 1.17–0.25$; $R^2 = 0.65$; $p < 0.005$; Fig. 3d).

For $^{210}Pb_{ex}$ at uncultivated sites the DMM and at cultivated sites the MBM with and without tillage component were applied. The estimates of the MBM2 correlate well with MODERN (Spearman $r = 0.9$) even though the MODERN estimates are considerably lower for the cultivated sites (approximately 20 t ha^{-1} yr^{-1}). The magnitude of erosion rates assessed with MODERN is closer to the one assessed with ^{137}Cs.

3.4.2. Soil redistribution estimates based on different FRNs

^{137}Cs and $^{239+240}$Pu based soil erosion rates correlate well (Fig. 4), and, if the particle size correction factor is considered for ^{137}Cs, then the estimates are also within the same order of magnitude. Without considering the preferential transport of ^{137}Cs, ^{137}Cs based soil erosion rates are overestimated by a factor of 2 as compared to the $^{239+240}$Pu based rates ($y = 2.03x–2.06$; $R^2 = 0.68$; $p < 0.0001$).

Between $^{210}Pb_{ex}$ and ^{137}Cs based rates, the R^2 of the regression is higher. However, the high R^2 results from the clustering of the data and as a consequence the regression is not significant ($p = 0.68$). Even the generally lower (compared to the estimates with MBM2) $^{210}Pb_{ex}$ estimates with MODERN are higher compared to the ^{137}Cs estimates (regression coefficient of 1.5). This could be due to the fact that no particle size correction factor could be estimated for $^{210}Pb_{ex}$. But attention should also be given to the different interpretation of the results provided by the $^{210}Pb_{ex}$ technique. $^{210}Pb_{ex}$ inventories in soils are likely to be more sensitive to the recent changes caused by soil movement (Mabit et al., 2014; Rabesiranana et al., 2016; Walling et al., 2003), because of its continuous input and its shorter half-life compared to the other FRNs. In the following we decided not to report $^{210}Pb_{ex}$ based soil redistribution estimates because of its high uncertainty. Uncertainty even amplified during the conversion of inventories to soil redistribution estimates. Under our experimental condition, data obtained with $^{210}Pb_{ex}$ were further not exploitable because of the high measurement uncertainty that emerged from the bulking of the sample soil profiles.

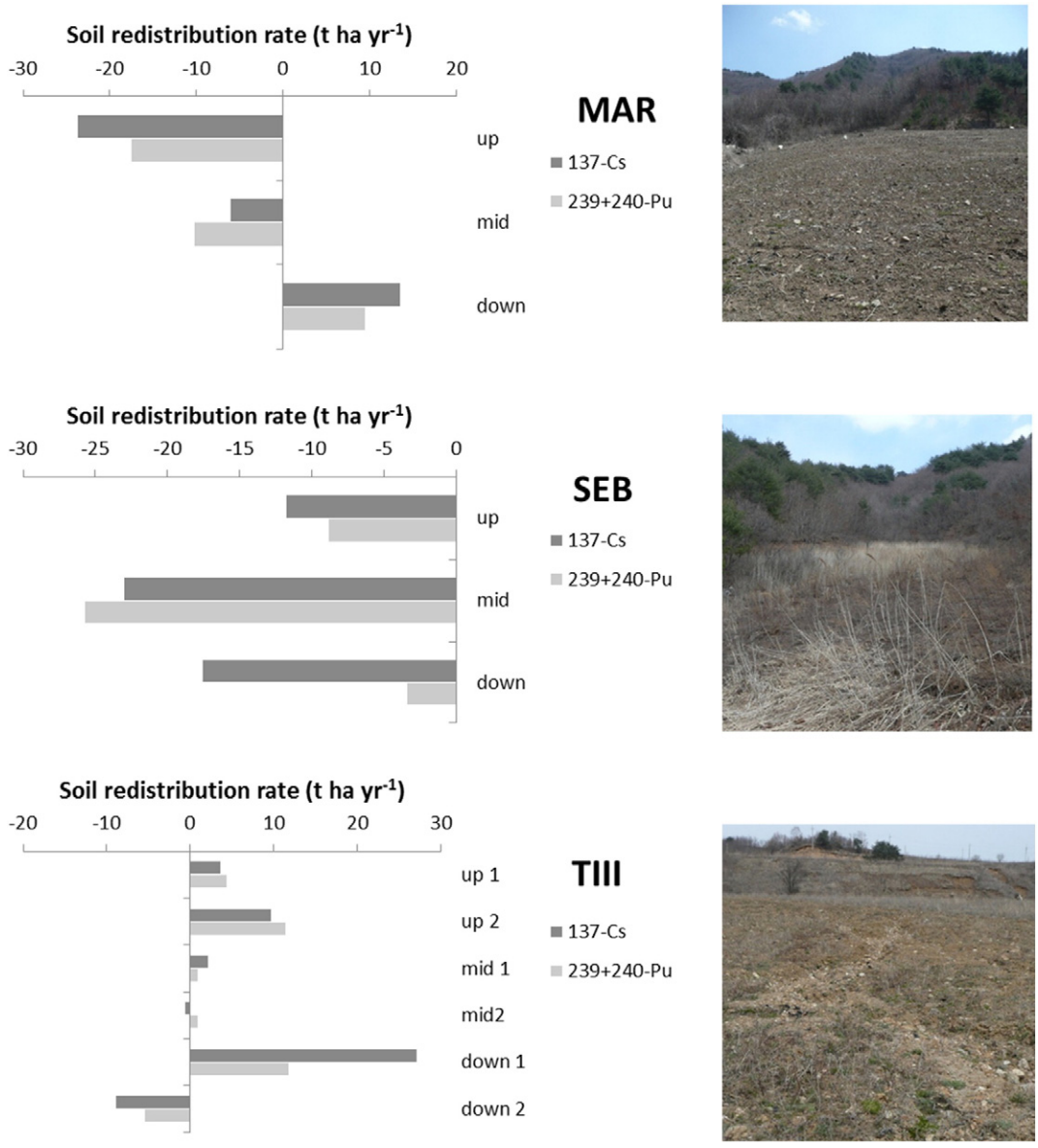

Fig. 5. Example of soil redistribution assessment for three specific transects with ^{137}Cs and $^{239+240}$Pu (MAR = recently deforested maize field, SEB = cabbage field, TIII = slope transect from a forest to an abandoned field).

High small scale heterogeneity in combination with a high measurement uncertainty may limit the use of $^{210}Pb_{ex}$ as soil redistribution tracer as has been already highlighted by Mabit et al. (2009).

3.4.3. Soil redistribution rates at different land use types and landscape positions

For the comparison of soil redistribution rates coming from different FRNs, we used MODERN except for ^{137}Cs for which we used the PDM in the case of uncultivated sites and the MBM2 for the cultivated ones. According to ^{137}Cs based soil redistribution estimates both uncultivated slope transects in the forest show relatively moderate erosion rates (Meusburger et al., 2013). Except for two sites with strong deviations of ^{137}Cs and $^{239+240}Pu$, the deviations are within the inner variability values observed at the reference site. The ^{137}Cs average erosion and sedimentation rates for the forest are −2.9 and 2.9 t ha^{-1} yr^{-1}, respectively. The $^{239+240}Pu$ estimates are slightly higher with −3.9 and 3.6 t ha^{-1} yr^{-1} for erosion and sedimentation magnitudes, respectively.

Transect MAR is located on a maize field that was deforested in 2006, only 4 years prior to sampling. Clearly all the FRNs show a soil redistribution from up- to downslope with very high erosion rates (−23.8, −17.5 t ha^{-1} yr^{-1} for ^{137}Cs and $^{239+240}Pu$, respectively) for the uppermost sampling site (Fig. 5). The transect SEB is cultivated since the 70s with cabbage in rotation with other vegetables. A clear depletion of the FRNs compared to the reference site with average erosion rates of −17.5 and −12.7 t ha^{-1} yr^{-1} for ^{137}Cs and $^{239+240}Pu$ is visible. Other erosion studies on dryland fields in the Kangwon Province show similar high values. For instance, Jung et al. (2003) found an average erosion rate of −47.5 t ha^{-1} yr^{-1}, and Choi et al. (2011) reported measured plot erosion rates between −4.2 t ha^{-1} yr^{-1} and −29.6 t ha^{-1} yr^{-1} for potato, and −3.3 t ha^{-1} yr^{-1} and −81.6 t ha^{-1} yr^{-1} for radish. However, the net soil erosion rates assessed with the FRNs are approximately one half of the gross erosion rates estimated with RUSLE in the same catchment ranging from −30.6 to −54.8 t ha^{-1} yr^{-1} (Arnhold et al., 2014).

The transitional transect with a change from forest to arable field sites exhibited an interesting pattern (Fig. 5). It is common practice in the catchment that those high soil losses are compensated by the addition of top soil from neighboring forests. The two uppermost points of transect III are located in an undisturbed (judged from visual inspection of the soil profile) forest. Here, we observe slightly higher inventories most likely due to sedimentation from upslope material. The next two sampling points are located at the border of the forest where soil has been removed. Even though soil was removed here the observed inventory is still close to the reference inventory. Like the two upslope located sampling point these sites were most likely affected by sedimentation before the soil removal. The next point is located at the upslope part of the field and we clearly observe the increased inventory due to the input of forest topsoil material. The lower part of the field is depleted in FRN and most likely did not receive considerable amounts of topsoil from upslope. Another transect is also located on a field that was upgraded with forest soil and recently abandoned. While the added top soil was eroded again, in the depth of 10 to 14 cm the remains of a former added ^{137}Cs and organic matter rich layer could be measured and observed in the field (Fig. 6). In this case the anthropogenic soil removal could not be reconstructed and thus soil erosion rates could not be assessed.

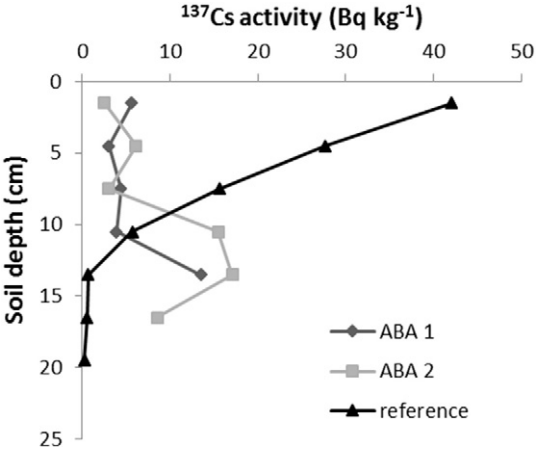

Fig. 6. ^{137}Cs depth profiles for two abandoned sites (ABA) that have been upgraded with forest topsoil.

4. Conclusion

This study set out to determine the origin and suitability of three FRNs (i.e. ^{137}Cs, $^{210}Pb_{ex}$ and $^{239+240}Pu$) as soil erosion tracers. As test area, the multiple land-use catchment Haean (close to the demilitarized zone in South Korea) affected by high erosion rates during the monsoon season was investigated.

Through the combination of $^{239+240}Pu$ with ^{137}Cs the origin of the fallout could be determined. Both $^{240}Pu/^{239}Pu$ atomic ratios and $^{239+240}Pu/^{137}Cs$ activity ratios were close to the global fallout and showed no sign of Pu input due to the nuclear bomb testing of North Korea. However, the depth profile of the $^{239+240}Pu/^{137}Cs$ activity ratios in the reference sites showed some interesting variation, with lower ratios in the top soil increments that can be attributed to higher migration rates of $^{239+240}Pu$ compared to ^{137}Cs. A further interesting aspect of the activity ratios is that they differ between bulk samples of erosion and sedimentation sites. Compared to the global fallout ratio the erosion sites are depleted in ^{137}Cs and the sedimentation sites slightly enriched. We interpret this deviation as a result of a more pronounced preferential transport of ^{137}Cs, which binds predominantly to fine soil particles. The aspect of preferential transport of ^{137}Cs and the parametrisation of the particle size correction factor (P) to account for the problem always poses an obstacle for soil erosion assessment. Here a new approach to parameterize P for its application with ^{137}Cs is suggested. In case the $^{239+240}Pu/^{137}Cs$ activity ratios are available a systematic shift of the ratio between erosion, sedimentation and reference sites may indicate preferential transport. The ratio between the $^{239+240}Pu/^{137}Cs$ activity ratio of the mobilized/deposited and the reference soil may serve as a proxy for the particle size correction factor P and P′ (in case of deposition). Following this approach - and taking into account the resulting P for ^{137}Cs - yields comparable estimates of soil redistribution between ^{137}Cs and $^{239+240}Pu$ in our study site. These first results on the parametrization of the particle size correction factor via the $^{239+240}Pu/^{137}Cs$ activity ratio are promising, but further field studies need to be carried out under different agro-environmental conditions in order to support this approach. The magnitude of P clearly highlights the importance of preferential transport of FRNs, which would deserve more attention in future studies.

The erosion assessments accomplished with different conversion models showed that in the case of ^{137}Cs, all models including the newly introduced MODERN yield similar results. For $^{210}Pb_{ex}$ and $^{239+240}Pu$ deviations between the different conversion models and FRNs were observed that were smallest for MODERN. Congruent with other studies measurement uncertainties of $^{210}Pb_{ex}$ represented a major obstacle for its application. The uncertainty level was further enhanced because large volumes of soil were composited for the analysis in this study. Thus, in the case of $^{210}Pb_{ex}$ we suggest to analyse depth incremental samples not only at the reference sites but also at sampling sites. Independent of the FRN and the conversion model used, there is a clear indication of very high erosion rates for cultivated sites with maximum erosion rates above 25 t ha^{-1} yr^{-1}. These values exceed by far the soil erosion rates of the very steep forested slopes in the catchment and are threatening to limit the agricultural resource soil.

Overall, the comparison among the different FRN highlights the suitability of $^{239+240}Pu$ through (i) reduced initial spatial variability, (ii) less

preferential transport and (iii) the possibility to gain information regarding the origin of the fallout. However, since the mobility i. e. vertical migration and lateral transport during water erosion of $^{239+240}$Pu in soils obviously differs from that of ^{137}Cs, there is a clear need for a wider agro-environmental testing of $^{239+240}$Pu and related conversion models to generate an improved understanding and thus assist the further development and improvement of conversion models such as MODERN.

Acknowledgements

The study was supported by the Swiss National Science Foundation and the National Research Foundation of Korea through the Strategic Korean-Swiss Cooperative Program (2009-83527) and has been finalized in the frame of the IAEA Coordinated Research Project (CRP) on '*Nuclear techniques for a better understanding of the impact of climate change on soil erosion in upland agro-ecosystems*' (D1.50.17).

Appendix A. Supplementary data

Supplementary data to this article can be found online at http://dx.doi.org/10.1016/j.scitotenv.2016.06.035.

References

Alewell, C., Meusburger, K., Juretzko, G., Mabit, L., Ketterer, M., 2014. Suitability of $^{239+240}$Pu as a tracer for soil erosion in alpine grasslands. Chemosphere 103, 274–280.

Arata, L., Alewell, C., Frenkel, E., A'Campo-Neuen, A., Iurian, A.-R., Ketterer, M.E., et al., 2016a. Modelling deposition and erosion rates with RadioNuclides (MODERN) – part 2: a comparison of different models to convert $^{239+240}$Pu inventories into soil redistribution rates at unploughed sites. J. Environ. Radioact. 162–163, 97–106.

Arata, L., Meusburger, K., Frenkel, E., A'Campo-Neuen, A., Iurian, A.-R., Ketterer, M.E., et al., 2016b. Modelling deposition and erosion rates with RadioNuclides (MODERN) – part 1: a new conversion model to derive soil redistribution rates from inventories of fallout radionuclides. J. Environ. Radioact. 162–163, 45–55.

Arnhold, S., 2012. Soil erosion and conservation potential of row crop farming in mountainous landscapes of South Korea. Bayreuth Graduate School of Mathematical and Natural Sciences (BayNAT). PhD.University Bayreuth, Bayreuth, p. 91

Arnhold, S., Lindner, S., Leeb, B., Martin, E., Kettering, J., Seo, B., et al., 2014. Conventional and organic farming: soil erosion and conservation potential for row crop cultivation. Geoderma 89-105.

Choi, J., Choi, Y., Lim, K., Shin, Y., 2011. Soil erosion measurement and control techniques. In: Chung, N., Kim, W., Kim, H., Kim, J., Eom, K., Lee, I. (Eds.), International Workshop on Newly Developed Innovative Technology for Soil and Water Conservation.

Choppin, G.R., 1988. Humics and radionuclide migration. Radiochim. Acta 44–45, 23–28.

Everett, S.E., Tims, S.G., Hancock, G.J., Bartley, R., Fifield, L.K., 2008. Comparison of Pu and ^{137}Cs as tracers of soil and sediment transport in a terrestrial environment. J. Environ. Radioact. 99, 383–393.

Fukuyama, T., Onda, Y., Takenaka, C., Walling, D.E., 2008. Investigating erosion rates within a Japanese cypress plantation using Cs-137 and Pb-210(ex) measurements. J. Geophys. Res. Earth Surf. 113.

Hakonson, T.E., Watters, R.L., Hanson, W.C., 1981. The transport of plutonium in terrestrial ecosystems. Health Phys. 40, 63–69.

Hardy, E.P., Krey, P.W., Volchok, H.L., 1973. Global inventory and distribution of fallout plutonium. Nature 241, 444–445.

He, Q., Walling, D.E., 1996. Interpreting particle size effects in the adsorption of ^{137}Cs and unsupported ^{210}Pb by mineral soils and sediments. J. Environ. Radioact. 30, 117–137.

Hirose, K., Kim, C.K., Kim, C.S., Chang, B.W., Igarashi, Y., Aoyama, M., 2004. Wet and dry deposition patterns of plutoniumin Daejeon, Korea. Sci. Total Environ. 332, 243–252.

Hodge, V., Smith, C., Whiting, J., 1996. Radiocesium and plutonium: still together in "background" soils after more than thirty years. Chemosphere 32, 2067–2075.

Iurian, A.R., Mabit, L., Cosma, C., 2014. Uncertainty related to input parameters of Cs-137 soil redistribution model for undisturbed fields. J. Environ. Radioact. 136, 112–120.

Jung, B.-J., Lee, H.-J., Jeong, J.-J., Owen, J., Kim, B., Meusburger, K., et al., 2012. Storm pulses and varying sources of hydrologic carbon export from a mountainous watershed. J. Hydrol. 440–441, 90–101.

Jung, K., Son, Y., Hur, S., Ha, S., Jang, Y., Jung, P., 2003. Estimation of national wide soil loss with soil type. National Academy of Agricultural Science (NAAS).

Kelley, J.M., Bond, L.A., Beasley, T.M., 1999. Global distribution of Pu isotopes and ^{237}Np. Sci. Total Environ. 237-238, 483–500.

Ketterer, M.E., Watson, B.R., Matisoff, G., Wilson, C.G., 2002. Rapid dating of recent aquatic sediments using Pu activities and Pu-240/Pu-239 as determined by quadrupole inductively coupled plasma mass spectrometry. Environ. Sci. Technol. 36, 1307–1311.

Ketterer, M.E., Zheng, J., Yamada, M., 2011. Applications of Transuranics as Tracers and Chronometers in the Environment. Berlin: Springer-Verlag, Berlin.

Kim, C.S., Lee, M.H., Kim, C.K., Kim, K.H., 1998. Sr-90, Cs-137, Pu239 + 240 and Pu-238 concentrations in surface soils of Korea. J. Environ. Radioact. 40, 75–88.

Kwon, Y.S., Lee, H.Y., Han, J., Kim, W.H., Kim, D.J., Kim, D.I., et al., 1990. Terrain analysis of Haean Basin in terms of earth science. J. Korean Earth Sci. Soc. 11, 236–241.

Lal, R., Tims, S.G., Fifield, L.K., Wasson, R.J., Howe, D., 2013. Applicability of Pu-239 as a tracer for soil erosion in the wet-dry tropics of northern Australia. Nuclear Instruments & Methods in Physics Research Section B-Beam Interactions with Materials and Atoms 294, 577–583.

Lee, M.H., Lee, C.W., Boo, B.H., 1997. Distribution and characteristics of ^{239}, ^{240}Pu and ^{137}Cs in the soil of Korea. J. Environ. Radioact. 37, 1–16.

Liao, H.Q., Bu, W.T., Zheng, J., Wu, F.C., Yamada, M., 2014. Vertical distributions of radionuclides (Pu239 + 240, Pu-240/Pu-239, and Cs-137) in sediment cores of Lake Bosten in northwestern China. Environ. Sci. Technol. 48, 3840–3846.

Lu, N., Kung, K.S., Mason, C.F.V., Triay, I.R., Cotter, C.R., Pappas, A.J., et al., 1998. Removal of plutonium-239 and americium-241 from rocky flats soil by leaching. Environ. Sci. Technol. 32, 370–374.

Lujaniene, G., Plukis, A., Kimtys, E., Remeikis, V., Jankunaite, D., Ogorodnikov, B.I., 2002. Study of Cs-137, Sr-90, Pu-239,Pu-240, Pu-238 and Am-241 behavior in the Chernobyl soil. J. Radioanal. Nucl. Chem. 251, 59–68.

Mabit, L., Benmansour, M., Walling, D.E., 2008. Comparative advantages and limitations of the fallout radionuclides ^{137}Cs, ^{210}Pb$_{ex}$ and ^{7}Be for assessing soil erosion and sedimentation. J. Environ. Radioact. 99, 1799–1807.

Mabit, L., Klik, A., Benmansour, M., Toloza, A., Geisler, A., Gerstmann, U.C., 2009. Assessment of erosion and deposition rates within an Austrian agricultural watershed by combining (CS)-C-137, Pb-210(ex) and conventional measurements. Geoderma 150, 231–239.

Mabit, L., Meusburger, K., Fulajtar, E., Alewell, C., 2013. The usefulness of ^{137}Cs as a tracer for soil erosion assessment: a critical reply to parsons and Foster (2011). Earth Sci. Rev. 137, 300–307.

Mabit, L., Benmansour, M., Abril, J.M., Walling, D.E., Meusburger, K., Iurian, A.R., et al., 2014. Fallout ^{210}Pb$_{ex}$ as a soil and sediment tracer in catchment sediment budget investigations: a review. Earth Sci. Rev. 138, 335–351.

Meusburger, K., Mabit, L., Park, J.H., Sandor, T., Alewell, C., 2013. Combined use of stable isotopes and fallout radionuclides as soil erosion indicators in a forested mountain site, South Korea. Biogeosciences 10, 5627–5638.

O'Farrell, C.R., Heimsath, A.M., Kaste, J.M., 2007. Quantifying hillslope erosion rates and processes for a coastal California landscape over varying timescales. Earth Surf. Process. Landf. 32, 544–560.

Park, J.-H., Inam, E., Abdullah, M.H., Agustiyani, D., Duan, L., Hoang, T.T., et al., 2011. Implications of rainfall variability for seasonality and climate-induced risks concerning surface water quality in East Asia. J. Hydrol. 400, 323–332.

Parsons, A.J., Foster, I.D.L., 2011. What can we learn about soil erosion from the use of ^{137}Cs? Earth Sci. Rev. 108, 101–113.

Porto, P., Walling, D.E., 2012a. Using plot experiments to test the validity of mass balance models employed to estimate soil redistribution rates from (137)Cs and (210)Pb(ex) measurements. Appl. Radiat. Isot. 70, 2451–2459.

Porto, P., Walling, D.E., 2012b. Validating the use of Cs-137 and Pb-210(ex) measurements to estimate rates of soil loss from cultivated land in southern Italy. J. Environ. Radioact. 106, 47–57.

Porto, P., Walling, D.E., Ferro, V., Di Stefano, C., 2003. Validating erosion rate estimates provided by caesium-137 measurements for two small forested catchments in Calabria, southern Italy. Land Degrad. Dev. 14, 389–408.

Porto, P., Walling, D.E., Callegari, G., 2013. Using ^{137}Cs and ^{210}Pbex measurements to investigate the sediment budget of a small forested catchment in southern Italy. Hydrol. Process. 27, 795–806.

Preiss, N., Meliérè, M., Pourchet, M., 1996. A compilation of data on lead-210 concentration in surface air and fluxes at the air-surface and water-sediment interfaces. J. Geophys. Res. 101, 28847–28862.

Qiao, J.X., Hansen, V., Hou, X.L., Aldahan, A., Possnert, G., 2012. Speciation analysis of I-129, Cs-137, Th-232, U-238, Pu-239 and Pu-240 in environmental soil and sediment. Appl. Radiat. Isot. 70, 1698–1708.

Rabesiranana, N., Rasolonirina, M., Solonjara, A.F., Ravoson, H.N., Andriambololona, R., L., M., 2016. Assessment of soil redistribution rates by ^{137}Cs and ^{210}Pb$_{ex}$ in a typical Malagasy agricultural field. J. Environ. Radioact. 152, 112–118.

Ruidisch, M., Arnhold, S., Bernd, H., Christina, B., 2013a. Is ridge cultivation sustainable? A case study from the Haean catchment, South Korea. Applied and Environmental Soil Science 11.

Ruidisch, M., Kettering, J., Arnhold, S., Huwe, B., 2013b. Modeling water flow in a plastic mulched ridge cultivation system on hillslopes affected by south Korean summer monsoon. Agric. Water Manag. 116, 204–217.

Schimmack, W., Auerswald, K., Bunzl, K., 2001. Can Pu239 + 240 replace Cs-137 as an erosion tracer in agricultural landscapes contaminated with Chernobyl fallout? J. Environ. Radioact. 53, 41–57.

Shakhashiro, A., Mabit, L., 2009. Results of an IAEA inter-comparison exercise to assess ^{137}Cs and total ^{210}Pb analytical performance in soil. Appl. Radiat. Isot. 67, 139–146.

Sutherland, R.A., 1991. Cesium-137 and sediment budgeting within a partially closed drainage-basin. Zeitschrift Fur Geomorphologie 35, 47–63.

Sutherland, R.A., 1996. Caesium-137 soil sampling and inventory variability in reference locations: A literature survey. Hydrol. Process. 10, 43–53.

Teramage, M.T., Onda, Y., Wakiyama, Y., Kato, H., Kanda, T., Tamura, K., 2015. Atmospheric Pb-210 as a tracer for soil organic carbon transport in a coniferous forest. Environmental Science-Processes & Impacts 17, 110–119.

Tims, S.G., Everett, S.E., Fifield, L.K., Hancock, G.J., Bartley, R., 2010. Plutonium as a tracer of soil and sediment movement in the Herbert River, Australia. Nuclear Instruments & Methods in Physics Research Section B-Beam Interactions with Materials and Atoms 268, 1150–1154.

UNSCEAR, 2000. Sources and Effects of Ionizing Radiation. Vol. 1. United Nations, New York, p. 158 Annex C.

Wakiyama, Y., Onda, Y., Mizugaki, S., Asai, H., Hiramatsu, S., 2010. Soil erosion rates on forested mountain hillslopes estimated using Cs-137 and Pb-210(ex). Geoderma 159, 39–52.

Walling, D.E., He, Q., Appleby, P.G., 2002. Conversion models for use in soil-erosion, soil-redistribution and sedimentation investigations. In: Zapata, F. (Ed.), Handbook for the Assessment of Soil Erosion and Sedimentation using Environmental Radionuclides, pp. 111–164 The Netherlands.

Walling, D.E., Collins, A.L., Sichingabula, H.M., 2003. Using unsupported lead-210 measurements to investigate soil erosion and sediment delivery in a small Zambian catchment. Studies on Large Volume Landslides. 52, pp. 193–213.

Walling, D.E., Zhang, Y., Q, H., 2003. Conversion models and related software. guidelines for using fallout radionuclides to assess erosion and effectiveness of soil conservation strategies. IAEA-TECDOC-1741, pp. 125–148 Vienna.

Xu, Y.H., Qiao, J.X., Hou, X.L., Pan, S.M., 2013. Plutonium in soils from Northeast China and its potential application for evaluation of soil erosion. Sci. Report. 3.

Xu, Y.H., Qiao, J.X., Pan, S.M., Hou, X.L., Roos, P., Cao, L.G., 2015. Plutonium as a tracer for soil erosion assessment in Northeast China. Sci. Total Environ. 511, 176–185.

Yamada, M., Zheng, J., Wang, Z.L., 2006. Cs-137, Pu239 + 240 and Pu-240/Pu-239 atom ratios in the surface waters of the western North Pacific Ocean, eastern Indian Ocean and their adjacent seas. Sci. Total Environ. 366, 242–252.

Zhang, K., Pan, S., Xu, Y., Cao, L., Hao, Y., Wu, M., et al., 2015. Using $^{239+240}$Pu atmospheric deposition and a simplified mass balance model to re-estimate the soil erosion rate: a case study of Liaodong Bay in China. J. Radioanal. Nucl. Chem.

Zollinger, B., Alewell, C., Kneisel, C., Meusburger, K., Brandová, D., Kubik, P., et al., 2014. The effect of permafrost on time-split soil erosion using radionuclides (^{137}Cs, $^{239+240}$Pu, meteoric ^{10}Be) and stable isotopes (^{13}C) in the eastern Swiss Alps. J. Soils Sediments.

Van Pelt, S., Zobeck, R., Ritchie, T.M., TE, J.C.G., 2007. Validating the use of ^{137}Cs measurements to estimate rates of soil redistribution by wind. Catena 70, 455–464.